AIAA 2013-2140

Numerical investigation of temperature effects on properties of subsonic turbulent jets

Christophe Bogey* and **Olivier Marsden†**
Laboratoire de Mécanique des Fluides et d'Acoustique
UMR CNRS 5509, Ecole Centrale de Lyon
69134 Ecully, France

The influence of temperature on the flow and acoustic fields of high subsonic jets is investigated by computing one isothermal and three hot circular jets using large-eddy simulation. The jets have an identical velocity yielding a Mach number $M = u_j/c_a = 0.9$, and diameter-based Reynolds numbers $Re_D = u_j D/\nu_j$ between 2.5×10^4 and 10^5, where subscripts j and a denote inflow and ambient conditions. They are characterized by similar nozzle-exit boundary-layer parameters, including 9% of peak turbulence intensity. The isothermal jet is at a temperature $T_j = T_a$ and at $Re_D = 10^5$. The next two jets are at $T_j = 1.5T_a$ and $T_j = 2.25T_a$, and have the same diameter as the isothermal jet, leading to $Re_D = 5 \times 10^4$ and $Re_D = 2.5 \times 10^4$, respectively. The last jet is also at $T_j = 1.5T_a$, but its diameter is doubled in order to obtain $Re_D = 10^5$. In all cases, with rising temperature, the jets develop more rapidly with higher turbulence levels, and generate more noise at low frequencies and less noise at high frequencies in the flow direction, in agreement with corresponding measurements. The variations of the shear-layer properties and of the far-field pressure levels with T_j are however strongly dependent on the Reynolds number. For the jets at a constant diameter, due to the decrease in Re_D, the mixing layers spread more quickly with higher velocity fluctuations and length scales, and the overall sound intensity increases. For the hot jet at $Re_D = 10^5$, on the contrary, the flow field downstream of the nozzle does not change significantly with respect to the isothermal case, and a noise reduction is found as observed experimentally for high Reynolds number jets at $M > 0.7$.

I. Introduction

The effects of temperature are known to be significant on the aerodynamic and acoustic fields of subsonic turbulent jets. Unfortunately, they have been described and explained in varied, and sometimes contradictory, manners. This issue is due to the difficulties encountered experimentally for hot jets, but also to the fact that several jet flow parameters change with heating. To mention two important ones, increasing jet temperature at fixed diameter D and velocity u_j, hence at a constant acoustic Mach number $M = u_j/c_a$, reduces the jet density ρ_j, as well as its Reynolds number $Re_D = u_j D/\nu_j$, where c and ν are the speed of sound and kinematic molecular viscosity, and subscripts j and a denote inflow and ambient conditions, respectively. Consequently, both density and Reynolds number variation effects are expected to occur, and they cannot usually be easily distinguished from each other.

On the basis of works carried out over the past forty years, some trends have however been established concerning the influence of temperature on jet flows. Linear stability analyses conducted by Maslowe & Kelly[1] and Michalke[2] suggested that instability waves in plane and axisymmetric shear layers grow at a higher rate with rising temperature on the high-speed side of the shear layers. This result was confirmed by measurements performed by Davey & Roshko[3] for initially laminar mixing layers between streams of different densities. In the same way, Brown & Roshko[4] found that turbulent mixing layers spread slightly more quickly when the density of the high-velocity stream is reduced. A large amount of experimental data have also been obtained for heated and variable-density jets. Witze,[5] Lau,[6] Lepicovsky[7] and Kearney-Fischer *et al.*[8]

*CNRS Research Scientist, AIAA Senior Member & Associate Fellow, christophe.bogey@ec-lyon.fr
†Assistant Professor at Ecole Centrale de Lyon, olivier.marsden@ec-lyon.fr

noted that the potential core length of subsonic jets shortens with the jet temperature T_j. Lau[6] pointed out, in addition, that the value of the turbulence intensity at the end of the potential core does not vary much with temperature, but that its peak value, reached farther downstream, increases. On his side, Lepicovsky[7] reported that the shortening of the potential core is followed by a more rapid decay of the centerline velocity. These tendencies correspond to those observed for variable-density turbulent jets, see in Pitts,[9] Russ & Strykowski[10] and Amielh *et al.*[11] for example, and can therefore be attributed to the reduction of density in heated jets. Finally, in a series of experiments aimed at exploring aeroacoustic sound sources, Bridges & Wernet[12,13] and Bridges[14] provided centerline velocity profiles as well as two-dimensional flow fields for isothermal and hot jets. They also remarked[13] that turbulence energy is about ten per cent higher in heated jets than in the unheated case, and that the spectral shapes and two-point space-time correlations of velocity fluctuations are insensitive to temperature if the streamwise location is normalized relative to the potential core length.

Regarding the influence of temperature on jet noise, experimental results from the fifties and sixties were rather confusing. The sound intensity was found to decrease with reducing jet density in Lassiter & Hubbard,[15] and with increasing temperature in Plumbee *et al.*,[16] but it was not noticeably different for cold and hot jets in Rollin.[17] Moreover, Plumbee *et al.*[16] observed only minor changes in the spectra, whereas Rollin[17] pinpointed a shift of acoustic energy from high to low Strouhal numbers for the hot cases. Clarifications were given in the seventies. Measurements by Fisher *et al.*[18] demonstrated that heated jets are noisier than cold jets at Mach numbers lower than 0.7, but quieter at higher Mach numbers. Similar findings were reported for jets with decreasing density by Hoch *et al.*,[19] who also noted that noise is typically stronger at low frequencies but weaker at high frequencies. Shortly after, Tanna *et al.*[20] showed that an elevated temperature leads to a significant increase of low-frequency noise in the sideline direction for low-speed jets, but to a decrease of levels over the entire frequency range for high-speed jets. Tanna[21] then performed a systematic study of the effects of temperature on jet noise, supplying data which have so far been used as reference data, as was the case in Bridges & Brown[29] and Panda[22] for instance. Based on these data, at the Mach number of 0.9 which will be considered in the present paper, the reduction of the overall sound intensity due to heating appears to be negligible at an angle $\phi = 40^{\circ}$ relative to the jet direction, and to be progressively larger as ϕ deviates from 40°. At $\phi = 45^{\circ}$, a moderate increase and a strong decrease of noise levels are visible at low and high frequencies respectively, whereas at $\phi = 90^{\circ}$, all acoustic components are weakened according to measurements of Bridges & Wernet.[13] To understand the variations of jet noise features with temperature, theoretical developments have been carried out by Morfey,[23] Tester & Morfey[24] and Morfey *et al.*,[25] among others. They revealed that heating jets reduces the strength of the quadrupole sources existing in unheated jets due to the density lowering, while creating extra dipole sources associated with the presence of density fluctuations, whose noise scales with the sixth power of the jet velocity. This view has been widely accepted, but it was questioned a decade ago by Viswanathan[26] who argued that additional features in sound spectra of hot jets result in some cases from spurious facility noise and/or from Reynolds number effects when $\mathrm{Re}_D \lesssim 400,000$. A lively and ongoing discussion on that matter has ensued. Tester & Morfey[27] and Harper-Bourne[28] notably re-examined available experimental databases, and concluded that these still strongly indicate the generation of dipole sources by heating. Furthermore, in the light of the works of Bridges & Brown,[29] Zaman[30] and Karon & Ahuja,[31] the differences between measurements obtained using different facilities and/or nozzles most probably stem, contrary to the claims of Viswanathan,[26] from changes in nozzle-exit conditions and not from noise contamination. The variations of jet exit parameters such as the boundary-layer thickness and the peak turbulence intensity are indeed likely to cause significant alterations in the flow and far-field characteristics of subsonic jets, which was recently highlighted by the simulations of Bogey & Bailly,[32] Bogey *et al.*[33] and Bogey & Marsden.[34]

To find new arguments concerning the effects of temperature on jets, complementing those issued from experimental databases, it seems interesting to turn to numerical simulations. Obviously, given the controversy mentioned above on the reliability of measurements, there is a need for high-fidelity computations providing accurate solutions. Over the past years, the feasibility of performing large-eddy simulations (LES) of variable-density jets has for instance been shown by Wang *et al.*[35] and Foysi *et al.*,[36] who calculated round and plane jets at Reynolds numbers below 32,000. The approach consisting in computing jet noise directly from the compressible Navier-Stokes equations has also reached maturity, see the review papers by Colonius & Lele,[37] Bailly & Bogey[38] and Wang *et al.*,[39] as well as the most recent studies of the present authors on isothermal jets.[32–34,40–42] This approach has been applied to non-isothermal free shear flows, such as mixing layers by Fortuné *et al.*[43] and Sharma & Lele,[44] axisymmetric jets by Lesshafft *et al.*[45] and round jets by

Bodony & Lele,[46] for example. The results were in general consistent with experimental observations, but notable discrepancies were also recognized. In particular, Bodony & Lele[46] carried out LES at conditions matching those of the jets of Tanna[21] except for lower Reynolds numbers, and obtained, at a Mach number of 0.9, higher noise levels at wide radiation angles with heating, while Tanna[21] noted a reduction. They attributed this to the limited resolution of their LES using about 10^6 grid points, but initial condition and Reynolds number effects could also be involved.

In the present study, one isothermal and three hot round jets are computed by LES to investigate the influence of temperature on the flow and acoustic fields of turbulent high subsonic jets. The simulations are performed on a grid containing 252 million points using low-dissipation finite differences and relaxation filtering as subgrid dissipation. The jets have an identical initial velocity yielding an acoustic Mach number $\mathrm{M} = 0.9$, and Reynolds numbers Re_D between 2.5×10^4 and 10^5. In order to minimize initial condition effects, they are characterized, at the exit of a pipe nozzle of radius $r_0 = D/2$, by similar flow conditions, including mean velocity profiles corresponding to a laminar profile of thickness $\delta_0 = 0.15r_0$ and, thanks to the use of a boundary-layer trip-like excitation, 9% of peak turbulence intensity. The isothermal jet is that at a temperature $T_j = T_a$ and a Reynolds number $\mathrm{Re}_D = 10^5$ considered in Bogey *et al.*,[33,40–42] whose LES was shown to be of quality in terms of both discretization and physical dissipation of the turbulent scales. The first two hot jet are at $T_j = 1.5T_a$ and $T_j = 2.25T_a$, and have the same diameter as the isothermal jet, leading to lower values of Re_D. The third hot jet is also at $T_j = 1.5T_a$, but its diameter is adjusted in order to maintain $\mathrm{Re}_D = 10^5$. This set of simulations allows several objectives to be be pursued in this work. The first objective will be to provide a comprehensive and detailed description of the flow and sound fields of the jets. The next one will be to identify unambiguous trends with heating, and to compare them to published experimental and numerical results. Then, in order to better understand the effects of temperature on noise generation mechanisms, links between the trends observed for the turbulence properties and those for the acoustic levels will be sought. Finally, we will attempt to distinguish between temperature effects due to density and Reynolds number variations. In this way, the present LES should help to clarify the impact of temperature on jet noise databases.

The paper is organized as follows. The main characteristics of the jets and of the simulations, including numerical algorithm and computational parameters, are documented in section II. The nozzle-exit flow conditions, and the aerodynamic and acoustic fields obtained for the different jets, are described in section III. Finally, concluding remarks are given in section IV.

II. Parameters

In this section, the jet inflow conditions are first presented. The numerical methods and parameters are then briefly reported. They are identical to those used in recent jet simulations, which have been thoroughly described in previous references.[33,34,40–42] The simulation of the isothermal jet at $\mathrm{Re}_D = 10^5$ considered in the present study was moreover detailed in Bogey *et al.*,[40] in which a great amount of information about the boundary-layer tripping procedure, the discretization quality and the LES reliability is available.

A. Jet definition

One isothermal and three hot jets at a Mach number $\mathrm{M} = u_j/c_a = 0.9$ are investigated. They originate at $z = 0$ from a pipe nozzle of radius r_0 and length $2r_0$, whose lip is $0.053r_0$ thick. The ambient temperature and pressure are $T_a = 293$ K and $p_a = 10^5$ Pa. For all jets, the axial velocity profile at the pipe inlet is given by an approximated solution of the Blasius laminar boundary-layer profile. More precisely, a Pohlhausen's fourth-order polynomial profile of thickness $\delta_0 = 0.15r_0$, yielding a 99% velocity thickness $\delta_{99} = 0.12r_0$ and a momentum thickness $\delta_\theta = 0.018r_0$, is imposed.[32] Radial and azimuthal velocities are initially set to zero, pressure is set to p_a, and the temperature is determined by a Crocco-Busemann relation. In order to generate highly disturbed upstream conditions for the jets, whose initial state would otherwise be laminar, a trip-like forcing is applied to the boundary layers at $z = -0.95r_0$ inside the pipe by adding random low-level vortical disturbances decorrelated in the azimuthal direction. The excitation magnitudes are empirically chosen to obtain, at the pipe exit, mean velocity profiles remaining similar to the Blasius laminar profiles introduced at the pipe inlet, and peak turbulence intensities u'_e/u_j around 9% as in the tripped subsonic jets of Zaman,[47,48] which will be shown in section III.A. Pressure fluctuations of maximum amplitude 200 Pa random in both space and time are also added in the shear layers between $z = 0.25r_0$ and $z = 4r_0$ from $t = 0$

up to non-dimensional time $t = 12.5r_0/u_j$, in order to speed up the initial transitory period.

The main jet inflow parameters are collected in table 1. Two jet diameters are considered with the aim of distinguishing between the effects of density and viscosity variations, as was tried by Amielh *et al.*[11] for variable-density jets. The first jet is at ambient temperature, and has a diameter $D = 0.5$ cm giving a Reynolds number $\mathrm{Re}_D = 10^5$. The next two jets are at $T_j = 1.5T_a$ and $T_j = 2.25T_a$, and have the same diameter as the isothermal jet. The two temperatures lead to densities and molecular viscosities $\rho_j = 0.67\rho_a$ and $\nu_j = 2\nu_a$, and $\rho_j = 0.4\rho_a$ and $\nu_j = 4\nu_a$, respectively, and consequently to $\mathrm{Re}_D = 5 \times 10^4$ and $\mathrm{Re}_D = 2.5 \times 10^4$. At such low values, the jet flow and acoustic properties change significantly with the Reynolds number according to an earlier numerical study[42] dealing with isothermal jets. The last jet is also at a temperature $T_j = 1.5T_a$, but its diameter is doubled in order to obtain $\mathrm{Re}_D = 10^5$ as for the isothermal jet, thus minimizing Reynolds number effects. In this case, the trends observed with heating should correspond to those found experimentally for high-Reynolds-number jets, in which viscosity plays a negligible role.

Table 1. Jet inflow parameters: Mach number $\mathrm{M} = u_j/c_a$, temperature T_j/T_a, diameter D, Reynolds number $\mathrm{Re}_D = u_j D/\nu_j$, density ρ_j/ρ_a, kinematic molecular viscosity ν_j/ν_a, inlet boundary-layer momentum thickness δ_θ, and strength of the trip-like excitation α_{trip} (subscripts j and a denote inflow and ambient conditions, respectively).

M	T_j/T_a	D (cm)	Re_D	ρ_j/ρ_a	ν_j/ν_a	δ_θ/r_0	α_{trip}
0.9	1	0.5	10^5	1	1	0.018	0.045
0.9	1.5	0.5	5×10^4	0.67	2	0.018	0.0658
0.9	2.25	0.5	2.5×10^4	0.40	4	0.018	0.1215
0.9	1.5	1	10^5	0.67	2	0.018	0.0439

For completeness, the amplitude of the trip-like excitation applied to the jet boundary layers to reach $u'_e/u_j \simeq 9\%$ is provided in table 1. The coefficient α_{trip} specifying the forcing strength, refer to appendix A in Bogey *et al.*,[40] is set to values of 0.045, 0.0658 and 0.1215 for the jets at a constant diameter with increasing temperature. Thus, the lower the Reynolds number, the higher the magnitude of the forcing necessary to achieve a given level of nozzle-exit velocity disturbances, in agreement with previous findings.[42] For the hot jet at $\mathrm{Re}_D = 10^5$, the value of α_{trip} is equal to 0.0439, which is close to that used for the isothermal jet at an identical Reynolds number.

B. LES procedure and numerical methods

The LES are carried out using a solver of the three-dimensional filtered compressible Navier-Stokes equations in cylindrical coordinates (r, θ, z) based on low-dissipation and low-dispersion explicit schemes. The axis singularity is taken into account by the method of Mohseni & Colonius.[49] In order to alleviate the time-step restriction near the cylindrical origin, the derivatives in the azimuthal direction around the axis are calculated at coarser resolutions than permitted by the grid.[50] Fourth-order eleven-point centered finite differences are used for spatial discretization, and a second-order six-stage Runge-Kutta algorithm is implemented for time integration.[51] A sixth-order eleven-point centered filter[52] is applied explicitly to the flow variables every time step. Non-centered finite differences and filters are also used near the pipe walls and the grid boundaries.[32,53] The radiation conditions of Tam & Dong[54] are applied at all boundaries, with the addition at the outflow of a sponge zone combining grid stretching and Laplacian filtering.[55]

In the simulations, the explicit filtering is employed to remove grid-to-grid oscillations, but also as a subgrid high-order dissipation model to relax turbulent energy from scales at wave numbers close to the grid cut-off wave number while leaving larger scales mostly unaffected.[56–58] With this in mind, the reliability of the LES fields obtained for the isothermal jet of the present study has been assessed in Bogey *et al.*[40] based on the tranfer functions associated with molecular viscosity, relaxation filtering and time integration. Viscosity was shown to be the dominant dissipation mechanism for scales discretized at least by seven points per wavelength. The physics of the larger turbulent structures is therefore unlikely to be governed by numerical or subgrid-modeling dissipation. This allows in particular the effective flow Reynolds number not to be artificially decreased, and viscosity effects to be properly captured, as was the case in Bogey *et al.*[40] for isothermal jets at Re_D between 2.5×10^4 and 2×10^5. These remarks certainly equally hold in this work for the LES of the hot jets which are at Reynolds numbers equal to or lower than that of the isothermal jet.

C. Simulation parameters

As indicated in table 2, the LES are performed using a grid containing $n_r \times n_\theta \times n_z = 256 \times 1024 \times 962 = 252$ million points. There are 169 points along the pipe nozzle, 77 points within the jet radius, and 31 points inside the inlet boundary layers. The physical domain, excluding the eighty-point outflow sponge zone, extends axially down to $L_z = 25r_0$, and radially out to $L_r = 9r_0$.

Table 2. Simulation parameters: numbers of grid points n_r, n_θ and n_z, mesh spacings Δr at $r = r_0$, $r_0\Delta\theta$, and Δz at $z = 0$, extents L_r and L_z of the physical domain, radial position r_c of the far-field extrapolation surface, number of time steps n_{it} and time duration T ($^*n_{it} = 140,000$ and $Tu_j/r_0 = 320$ for the jet at $T_j = 1.5T_a$ and $\mathrm{Re}_D = 10^5$).

$n_r \times n_\theta \times n_z$	$\Delta r/r_0$	$r_0\Delta\theta/r_0$	$\Delta z/r_0$	L_r, L_z	r_c/r_0	n_{it}	Tu_j/r_0
$256 \times 1024 \times 962$	0.36%	0.61%	0.72%	$9r_0, 25r_0$	6.5	164,000*	375*

The mesh spacing is uniform in the azimuthal direction, with $r_0\Delta\theta = 0.0061r_0$. In the axial direction, the mesh spacing is minimum between $z = -r_0$ and $z = 0$, with $\Delta z = 0.0072r_0$. It increases upstream of $z = -r_0$, but also downstream of the nozzle at stretching rates lower than 1% allowing to reach $\Delta z = 0.065r_0$ between $z = 13.3r_0$ and $z = L_z = 25r_0$. In the radial direction, the mesh spacing is minimum around $r = r_0$, with $\Delta r = 0.0036r_0$. It is equal to $\Delta r = 0.292r_0$ close to the jet axis, to $\Delta r = 0.081r_0$ between $r = 3r_0$ and $r = 6.75r_0$, and finally to $\Delta r = 0.176r_0$ at $r = L_r = 9r_0$. Further details regarding the mesh spacings can be found in previous papers.[33,40]

The quality of the discretization of the isothermal jet of the present study has been discussed in Bogey *et al.*[40] The ratios between the integral length scales of the axial fluctuating velocity and the mesh spacings along the lip line were shown to fall between 4 and 10. The properties of the nozzle-exit turbulence and of the shear-layer flow fields were moreover found to be practically converged with respect to the grid. Based on these results, there seems little doubt that the grid resolution is also appropriate for the three hot jets computed in this work, which are at same or lower Reynolds numbers with respect to the isothermal case. Lower Reynolds numbers indeed lead to an increase of the integral length scales and to the weakening of the contribution of fine-scale turbulence, as illustrated by recent simulations.[42]

The simulation time, given in table 2, is equal to $320r_0/u_j$ for the jet at $T_j = 1.5T_a$ and $\mathrm{Re}_D = 10^5$, and to $375r_0/u_j$ for the three others. After the initial transitory period, density, velocity components and pressure are recorded from time $t = 100r_0/u_j$ along the jet axis, and on two surfaces at $r = r_0$ and $r = r_c = 6.5r_0$, at a sampling frequency allowing the computation of spectra up to a Strouhal number of $\mathrm{St}_D = fD/u_j = 20$, where f is the time frequency. The cylindrical surface surrounding the jets is located at $r = 6.5r_0$ because, as indicated previously, the radial mesh spacing is uniform for $3r_0 \leq r \leq 6.75r_0$ but then increases for $r \geq 6.75r_0$. The radial mesh spacing at $r = 6.5r_0$ furthermore yields a Strouhal number of $\mathrm{St}_D = fD/u_j = 6.9$ for an acoustic wave discretized by four points per wavelength. In the azimuthal direction, every fourth grid point is stored, allowing data post-processing to be performed up to an azimuthal mode $n_\theta = 128$, where n_θ is the dimensionless azimuthal wave number such that $n_\theta = k_\theta r$. The velocity spectra are evaluated from overlapping samples of duration $27.4r_0/u_j$. The flow statistics are determined from $t = 175r_0/u_j$, and they are averaged in the azimuthal direction. They can be considered to be well converged in view of the results obtained at intermediary stages of the LES for $t \geq 300r_0/u_j$.

The simulations have run using an OpenMP-based in-house solver, on 7 processors of a NEC SX-8 computer at a central processing unit (CPU) speed of around 36 Gflops, then on 32 processors of an IBM Power7 computer. A number of 100,000 time steps required 4,200 CPU hours in the former case, and 66,000 CPU hours in the latter. In both cases, about 60 GB of memory were necessary.

D. Far-field extrapolation

The LES near fields are propagated to the acoustic far field by solving the isentropic linearized Euler equations (ILEE) in cylindrical coordinates.[59] The extrapolation is performed from fluctuating velocities and pressure recorded in the LES on a surface at $r = 6.5r_0$ as mentioned above. Concerning the position of the surface, it can be noted that similar far-field results were obtained using two surfaces at $r = 5.25r_0$ and at $r = 7.25r_0$ in Bogey & Bailly[32] for an initially laminar jet. The data at $r = 6.5r_0$ are interpolated onto a cylindrical surface discretized by an axial mesh spacing of $\Delta z = 0.065r_0$. They are then imposed at the bottom boundary of the grid on which the ILEE are solved using the same numerical methods as in the LES. This grid contains

$845 \times 256 \times 1155$ points, and extends axially from $z = -16.6r_0$ to $58.2r_0$ and radially up to $r = 61.4r_0$. The grid spacings are uniform with $\Delta r = \Delta z = 0.065r_0$, yielding $\mathrm{St}_D = 8.6$ for an acoustic wave at four points per wavelength. After a propagation time of $t \simeq 60r_0/u_j$, pressure is recorded around the jets at a distance of $60r_0$ from $z = r = 0$, where far-field acoustic conditions are expected to apply according to the experiments of Ahuja *et al.*,[60] during a period of $195r_0/u_j$ for the jet at $T_j = 1.5T_a$ and $\mathrm{Re}_D = 10^5$, and of $250r_0/u_j$ for the others. Pressure spectra are evaluated using overlapping samples of duration $38r_0/u_j$, and they are averaged in the azimuthal direction.

III. Results

A. Nozzle-exit conditions

To give a brief description of the jet initial conditions, the profiles of mean and rms axial velocities calculated at the nozzle exit are represented in figures 1(a-b), and the main exit flow parameters are provided in table 3. As intended, the mean velocity profiles do not appreciably differ from the Blasius laminar profile imposed at the pipe-nozzle inlet, leading to boundary-layer momentum thicknesses $\delta_\theta(0) = 0.0185r_0 - 0.02r_0$ and shape factors $\mathrm{H} = 2.19 - 2.36$, and the turbulence intensity profiles closely resemble each other, all reaching a peak around $u'_e/u_j = 9.15\%$. The profiles are also shown to be comparable to those measured by Zaman[47,48] about $0.1r_0$ downstream of the exit section of a tripped jet at $\mathrm{Re}_D = 10^5$. These results indicate that the jets are initially highly disturbed but not fully turbulent, and that they are characterized by similar nozzle-exit conditions except for the temperature and the Reynolds number. Concerning the Reynolds number $\mathrm{Re}_\theta = u_j\delta_\theta(0)/\nu_j$ based on the boundary-layer momentum thickness, it is found to be approximately 940 for the two isothermal and hot jets at $\mathrm{Re}_D = 10^5$, and to be equal to 485 and 254 for the hot jets at $\mathrm{Re}_D = 5\times10^4$ and 2.5×10^4, respectively. At such values, viscosity effects are expected to be significant. Finally, the slight changes in nozzle-exit mean velocity profile observed for the present jets at various temperatures appear to depend essentially on the Reynolds number. Indeed, the lower the value of Re_θ, the larger the thickness of the exit boundary layer, and the smaller its associated shape factor, which is consistent with trends obtained for isothermal jets.[42]

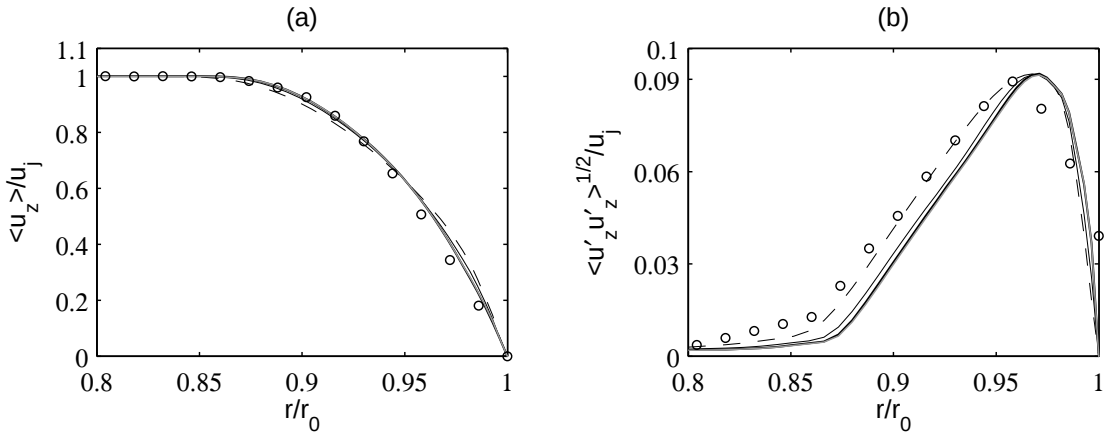

Figure 1. Profiles at $z = 0$ (a) of mean axial velocity $< u_z >$ and (b) of the rms values of fluctuating axial velocity u'_z for: ——— $T_j = T_a$ and $\mathrm{Re}_D = 10^5$, ——— $T_j = 1.5T_a$ and $\mathrm{Re}_D = 5\times10^4$, – – – $T_j = 2.25T_a$ and $\mathrm{Re}_D = 2.5 \times 10^4$, ——— $T_j = 1.5T_a$ and $\mathrm{Re}_D = 10^5$; ∘ measurements of Zaman[47,48] for a tripped jet at $\mathrm{Re}_D = 10^5$ about $0.1r_0$ downstream of the exit plane.

As in our previous studies on tripped jets,[33,34,40–42] the properties of the jet initial disturbances are examined by computing spectra of the fluctuating axial velocity at a position close to the nozzle exit to avoid the turbulence features being strongly affected by the mixing-layer development. The spectra estimated at $r = r_0$ and $z = 0.4r_0$ are represented as a function of the Strouhal number $\mathrm{St}_D = fD/u_j$ in figure 2(a), and of the azimuthal mode n_θ in figure 2(b). Their overall shapes are roughly similar in the four cases, and correspond, as was discussed in a specific note[41] on that matter, to the spectral shapes encountered for turbulent wall-bounded flows. It is also striking to see that the spectra obtained for the jets at a constant diameter change with heating, whereas those for the isothermal jet and for the hot jet at same $\mathrm{Re}_D = 10^5$ are

Table 3. Jet nozzle-exit conditions: momentum thickness $\delta_\theta(0)$ and shape factor H of the boundary layer, Reynolds number $\mathrm{Re}_\theta = u_j\delta_\theta(0)/\nu_j$ and peak turbulence intensity u'_e/u_j, and axial and azimuthal integral length scales $L_{uu}^{(z)}$ and $L_{uu}^{(\theta)}$ calculated from velocity u'_z at $r = r_0$ and $z = 0.4r_0$.

T_j/T_a	Re_D	$\delta_\theta(0)/r_0$	H	Re_θ	u'_e/u_j	$L_{uu}^{(z)}/r_0$	$L_{uu}^{(\theta)}/r_0$
1	10^5	0.0185	2.36	943	9.18%	0.058	0.013
1.5	5×10^4	0.0191	2.29	485	9.14%	0.068	0.014
2.25	2.5×10^4	0.0200	2.19	254	9.17%	0.077	0.021
1.5	10^5	0.0185	2.36	941	9.15%	0.055	0.012

nearly superimposed. In the former case, in agreement with observations made when the Reynolds number of isothermal jets is reduced,[42] a higher temperature results in weaker high-frequency components at Strouhal numbers $\mathrm{St}_D \gtrsim 3$ and azimuthal modes $n_\theta \gtrsim 60$, and conversely in stronger low-frequency components. The axial and azimuthal integral length scales consequently increases from $L_{uu}^{(z)} = 0.058r_0$ and $L_{uu}^{(\theta)} = 0.013r_0$ at $T_j = T_a$ up to $L_{uu}^{(z)} = 0.077r_0$ and $L_{uu}^{(\theta)} = 0.021r_0$ at $T_j = 2.25T_a$, as reported in table 3. These results demonstrate that the Reynolds number is the key factor influencing the structure of the jet initial turbulence, and that the temperature itself is of minor importance here.

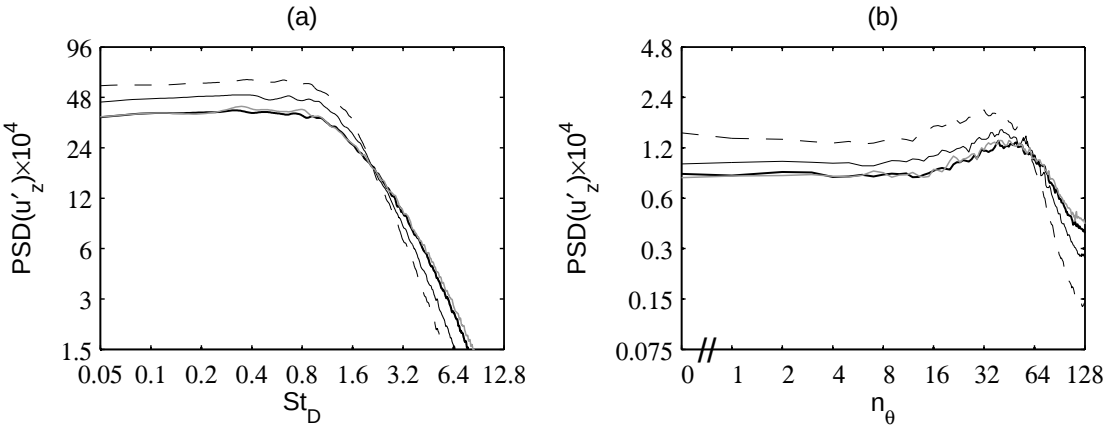

Figure 2. Power spectral densities (PSD) normalized by u_j of fluctuating velocity u'_z at $r = r_0$ and $z = 0.4r_0$, as functions (a) of Strouhal number $\mathrm{St}_D = fD/u_j$ and (b) of azimuthal mode n_θ for: ——— $T_j = T_a$ and $\mathrm{Re}_D = 10^5$, ——— $T_j = 1.5T_a$ and $\mathrm{Re}_D = 5\times10^4$, – – – $T_j = 2.25T_a$ and $\mathrm{Re}_D = 2.5\times10^4$, ——— $T_j = 1.5T_a$ and $\mathrm{Re}_D = 10^5$.

B. Shear-layer development

To provide a first insight into the early stage of development of the jet shear layers, vorticity fields obtained from the pipe-nozzle exit up to $z = 3r_0$ are represented in figures 3(a-d). Temperature is found to have varying effects depending on the Reynolds number. With respect to the isothermal jet in figure 3(a), the shear layers appear to spread more rapidly with stronger large-scale structures and weaker fine-scale turbulence for the hot jets at decreasing Reynolds numbers in figures 3(b-c), whereas this does not seem to be the case for the hot jet at $\mathrm{Re}_D = 10^5$ in figure 3(d). For the jet at $T_j = 2.25T_a$ and $\mathrm{Re}_D = 2.5\times10^4$ in figure 3(c), in particular, the shear layer displays, near the nozzle exit, structures elongated in the streamwise direction, as typically observed in turbulent boundary layers. It seems to roll up around $z = 0.8r_0$, and exhibits, farther downstream, large-scale structures resembling the coherent vortical structures revealed by the flow visualizations of Brown & Roshko.[4]

The variations over $0 \le z \le 10r_0$ of the momentum thickness δ_θ of the mixing layer and of its spreading rate $\mathrm{d}\delta_\theta/\mathrm{d}z$ are presented in figures 4(a-b). For the three jets with the same diameter, the mixing layer develops more rapidly with rising temperature, in accordance with the vorticity fields of figures 3(a-c). Furthermore, the profiles of spreading rate change significantly in terms of both amplitude and shape. In the isothermal case, it increases nearly monotonically, and shows maximum values of about $\mathrm{d}\delta_\theta/\mathrm{d}z = 0.024$

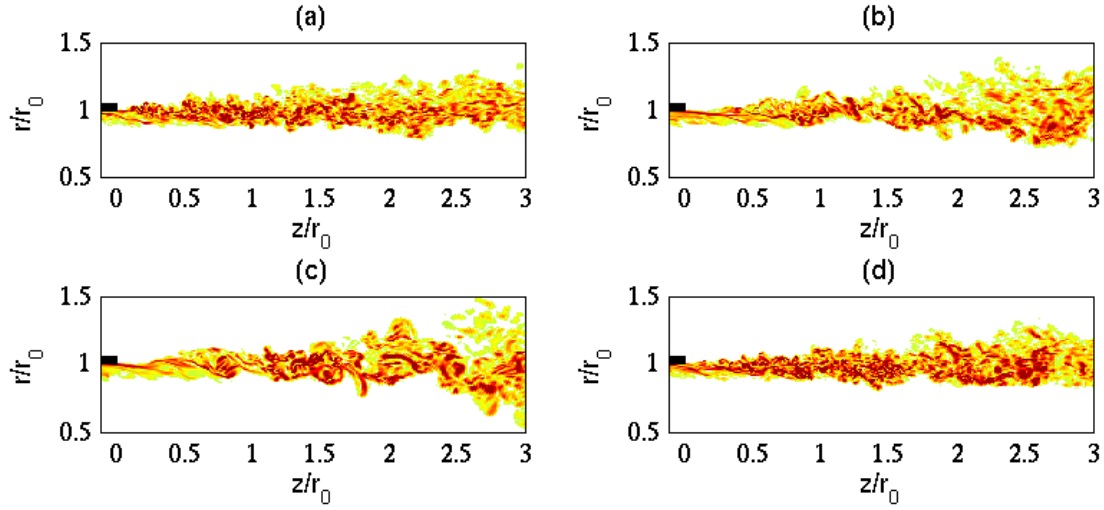

Figure 3. Snapshots in the (z,r) plane of vorticity norm $|\omega|$ downstream of the nozzle lip up to $z = 3r_0$ for: (a) $T_j = T_a$ and $\mathrm{Re}_D = 10^5$, (b) $T_j = 1.5T_a$ and $\mathrm{Re}_D = 5 \times 10^4$, (c) $T_j = 2.25T_a$ and $\mathrm{Re}_D = 2.5 \times 10^4$, (d) $T_j = 1.5T_a$ and $\mathrm{Re}_D = 10^5$. The colour scale ranges up to the level of $27u_j/r_0$. The nozzle lip is represented in black. Only $r \geq 0$ is shown.

between $z = 5r_0$ and $z = 10r_0$. At elevated jet temperatures, the spreading rates are higher, and reach pronounced peaks at axial locations moving upstream, of $\mathrm{d}\delta_\theta/\mathrm{d}z = 0.029$ at $T_j = 1.5T_a$ and $\mathrm{d}\delta_\theta/\mathrm{d}z = 0.0347$ at $T_j = 2.25T_a$, see in table 4. For the two jets at $\mathrm{Re}_D = 10^5$, the mixing layer also develops more quickly in the hot case than in the isothermal case, leading to a maximum spreading rate of 0.0272 at $T_j = 1.5T_a$, but the profiles of spreading rate do not differ significantly, especially in the region downstream of the nozzle exit. Therefore, it appears that a higher temperature enhances the development of the shear layers. The increase in spreading rates is however moderate, in agreement with the experimental data of Brown & Roshko[4] for variable-density turbulent mixing layers and of Panda[22] for hot jets at M = 0.9, and is more marked at large axial distances to the nozzle. The latter finding is in line with the measurements of Lau[6] who noted that heating jets at a velocity $u_j = 0.5c_j$ up to $T_j/T_a = 2.32$ results in negligible changes to the radial distribution of the Mach number up to $z = 8r_0$. This, in turn, indicates that the much stronger mixing-layer spreading obtained immediately downstream of the nozzle for the diameter-fixed jets at decreasing Re_D and Re_θ is due for a very large part to Reynolds number effects. This assertion is furthermore supported by the trends previously described for isothermal jets[42] with Reynolds numbers Re_θ varying from 943 down to 254.

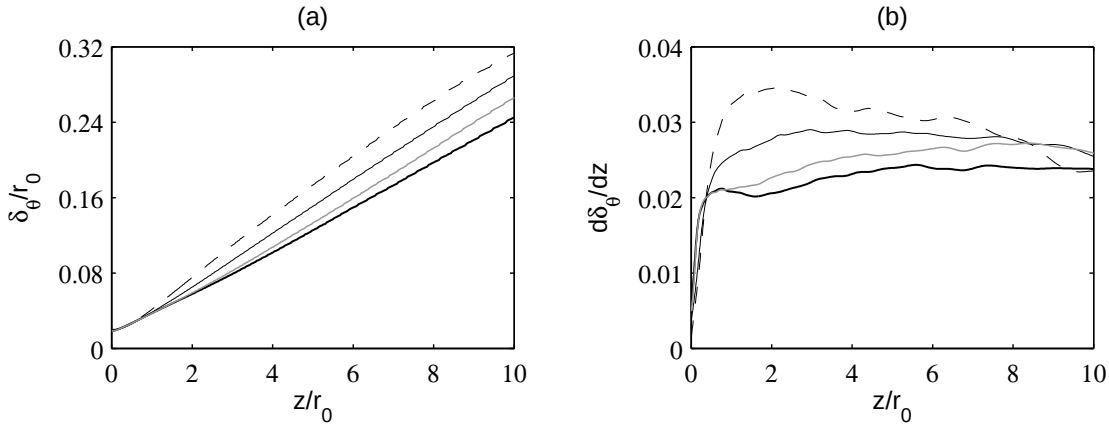

Figure 4. Variations (a) of shear-layer momentum thickness δ_θ and (b) of spreading rate $\mathrm{d}\delta_\theta/\mathrm{d}z$ for: ——— $T_j = T_a$ and $\mathrm{Re}_D = 10^5$, ——— $T_j = 1.5T_a$ and $\mathrm{Re}_D = 5 \times 10^4$, – – – $T_j = 2.25T_a$ and $\mathrm{Re}_D = 2.5 \times 10^4$, ——— $T_j = 1.5T_a$ and $\mathrm{Re}_D = 10^5$.

The variations between $z = 0$ and $z = 10r_0$ of the peak rms values of axial, radial and azimuthal

Table 4. Peak values of mixing-layer spreading rate and of turbulence intensities in the jets.

T_j/T_a	Re_D	$\mathrm{d}\delta_\theta/\mathrm{d}z$	$<u_z'^2>^{1/2}/u_j$	$<u_r'^2>^{1/2}/u_j$	$<u_\theta'^2>^{1/2}/u_j$	$<u_r'u_z'>^{1/2}/u_j$
1	10^5	0.0243	15.4%	11.2%	13.0%	9.3%
1.5	5×10^4	0.0290	17.1%	12.7%	14.4%	10.5%
2.25	2.5×10^4	0.0347	18.6%	14.0%	15.4%	11.7%
1.5	10^5	0.0272	16.0%	11.6%	13.3%	9.6%

velocities u_z', u_r' and u_θ' and of the maximum Reynolds shear stress $<u_r'u_z'>$ are displayed in figures 5(a-d). They follow trends which are similar to those detailed above for the mixing-layer spreading rate. For the jets at a constant diameter, with rising temperature, a hump progressively emerges around $z = 2r_0$ in the profiles of turbulence intensities. Consequently, the peak values become higher, and are equal, at the three temperatures considered, to 15.4%, 17.1% and 18.6% for u_z' and 11.2%, 12.7% and 14% for u_r', refer to table 4 for the other velocity components. For the two jets at $\mathrm{Re}_D = 10^5$, the profiles look, on the contrary, very much alike. In this case, heating only results in a slight increase of the fluctuation levels, yielding, at $T_j = 1.5T_a$, maximum rms values of $0.16u_j$ for u_z' and $0.116u_j$ for u_r', see also in table 4. The strengthening of the peak turbulence intensities in the jets with the same diameter can therefore be attributed to Reynolds number effects.[42] It can finally be noted that at large distances from the nozzle, typically for $z > 8r_0$, the levels of velocity fluctuations are ordered by the temperature. This is true for instance in figure 5(a), where the rms velocity values at $z = 10r_0$ are found to be of 14.8% at $T_j = T_a$, 15.6% at $T_j = 1.5T_a$ and $\mathrm{Re}_D = 10^5$, 15.7% at $T_j = 1.5T_a$ and $\mathrm{Re}_D = 5\times10^4$, and 16.4% at $T_j = 2.25T_a$. This tendency, which will be discussed in the next section, is consistent with the experimental data obtained by Bridges & Wernet[13] for unheated and heated jets with the same velocity.

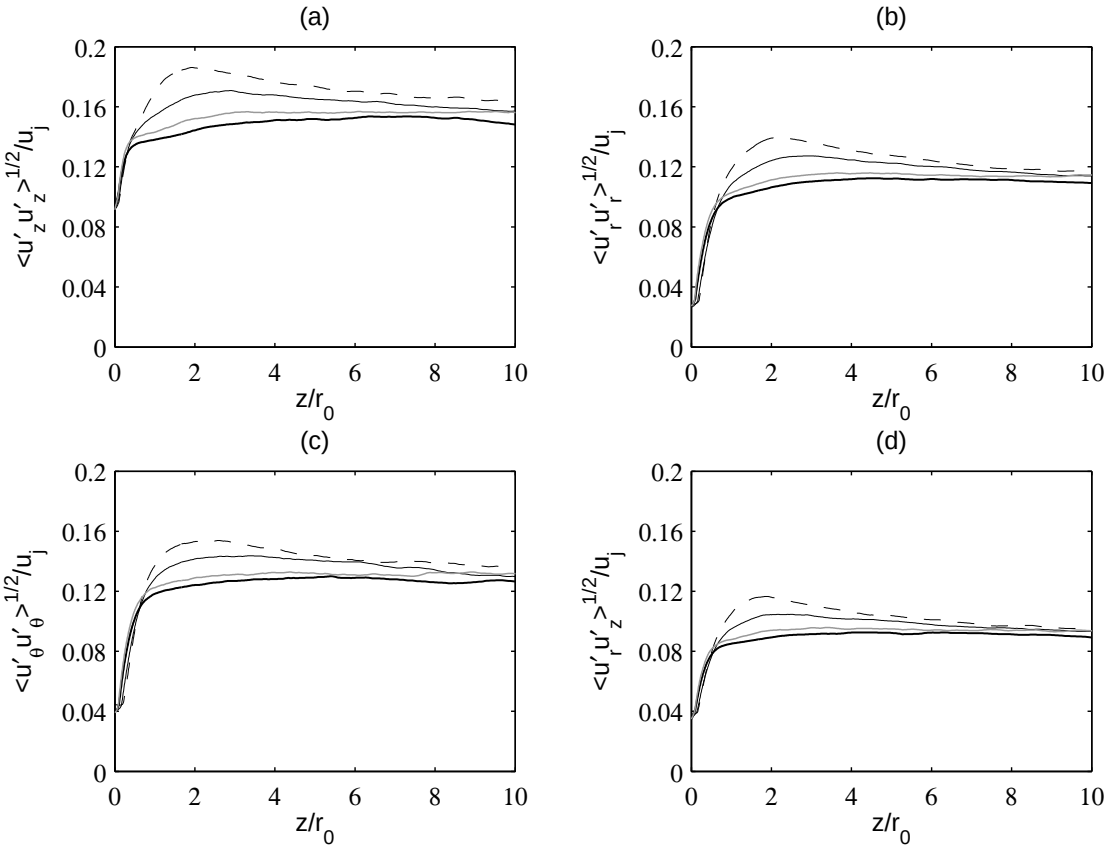

Figure 5. Variations of the peak rms values of fluctuating velocities (a) u_z', (b) u_r', (c) u_θ', and (d) of the peak magnitudes of Reynolds shear stress $<u_r'u_z'>$ for: ——— $T_j = T_a$ and $\mathrm{Re}_D = 10^5$, ——— $T_j = 1.5T_a$ and $\mathrm{Re}_D = 5\times10^4$, – – – $T_j = 2.25T_a$ and $\mathrm{Re}_D = 2.5\times10^4$, ——— $T_j = 1.5T_a$ and $\mathrm{Re}_D = 10^5$.

The axial and azimuthal integral length scales $L_{uu}^{(z)}$ and $L_{uu}^{(\theta)}$ estimated from velocity u'_z at $r = r_0$ along the lip line are plotted in figures 6(a-b). After a short period of decrease just downstream of the nozzle exit, they are both observed to grow fairly linearly with the axial distance, which is in agreement with the data available in the literature.[14,61,62]Heating visibly leads to larger integral length scales. However, as observed for the shear-layer momentum thickness in figure 4(a), the increase is important over the entire mixing layer for the jets with the same diameter, whereas it is significant only for $z \gtrsim 4r_0$ for the jets at a constant Reynolds number. This is obviously[42] due to the presence of strong Reynolds number effects in the former case, in which Re_θ is reduced from 934 down to 254 with rising temperature. As for the results found in the latter case, they bear similarity to those obtained for high-Reynolds-number jets by Bridges[14] and Wernet,[63] supporting the notion that heating does not significantly affect the turbulence length scales in the mixing layer near the nozzle, but causes a slight lengthening farther downstream.

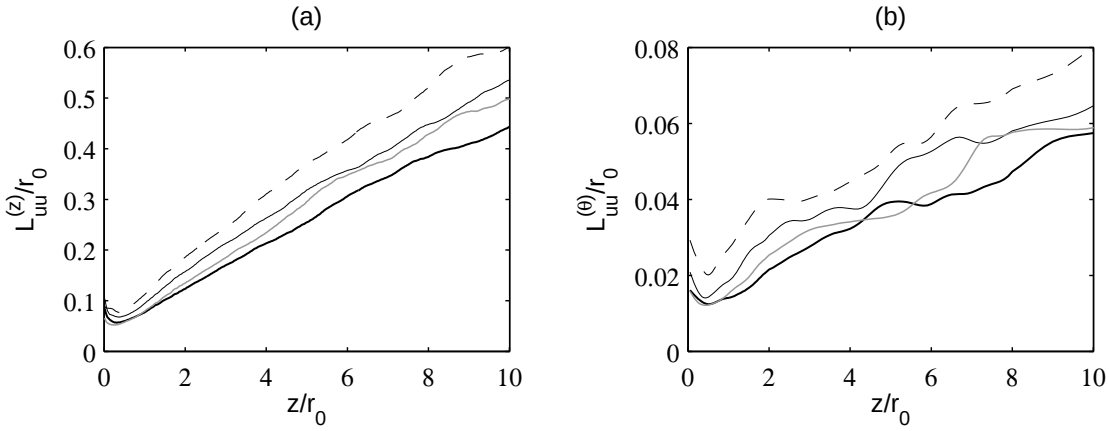

Figure 6. Variations of axial and azimuthal integral length scales (a) $L_{uu}^{(z)}$ and (b) $L_{uu}^{(\theta)}$ calculated from velocity u'_z at $r = r_0$ for: ——— $T_j = T_a$ and $\mathrm{Re}_D = 10^5$, ——— $T_j = 1.5T_a$ and $\mathrm{Re}_D = 5 \times 10^4$, − − − $T_j = 2.25T_a$ and $\mathrm{Re}_D = 2.5 \times 10^4$, ——— $T_j = 1.5T_a$ and $\mathrm{Re}_D = 10^5$.

C. Jet development

Vorticity fields obtained up to $z = 25r_0$ are represented in figures 7(a-d). With rising temperature, the jet mixing layers are seen to develop and merge more rapidly, in agreement with the increase in shear-layer spreading rate described in the previous section. Compare for instance figures 7(a) and 7(c): the end of the potential core is around $z = 15r_0$ for the isothermal jet, but around $z = 10r_0$ for the jet at $T_j = 2.25T_a$. Concerning the flow fields of the two jets at $T_j = 1.5T_a$ in figures 7(b-c), they do not seem fundamentally different.

The variations of the centerline mean axial velocity u_c and of the jet half-width $\delta_{0.5}$ are presented in figures 8(a-b). As the ratio T_j/T_a increases, the velocity decay and the jet spreading appear to start farther upstream, and then to occur faster. This leads to potential cores ending at $z_c = 15.9r_0$ for $T_j = T_a$, $z_c \simeq 13r_0$ for $T_j = 1.5T_a$, and $z_c = 10.6r_0$ for $T_j = 2.25T_a$, where $u_c(z_c) = 0.95u_j$, as reported in table 5. At $T_j = 1.5T_a$, the potential core lengths are more precisely of $z_c = 12.5r_0$ at $\mathrm{Re}_D = 5 \times 10^4$ and $z_c = 13.2r_0$ at $\mathrm{Re}_D = 10^5$, which indicates that the effects of the Reynolds number[42] on the mean flow of the present jets are relatively weak compared to those due to heating. The latter effects consist of a shortening of the potential core followed by a more rapid velocity decay, as was found in experiments dealing with heated jets, see for instance in Lau,[6] Lepicovsky,[7] Kearney-Fischer *et al.*[8] and Bridges.[14] For the sake of comparison, measurements provided by Bridges,[14] Fleury *et al.*[62] and Arakeri *et al.*[64] for cold, isothermal, slightly heated and heated jets at M = 0.9 and $\mathrm{Re}_D \geq 4 \times 10^5$ are depicted in figure 8(a). The data obtained for the first three jets fall near the velocity profile of the isothermal jet considered here, while those for the fourth jet at $T_j = 1.76T_a$ lie between the profiles of the jets at $T_j = 1.5T_a$ and of the jet at $T_j = 2.25T_a$. This result is remarkable given the differences in terms of jet diameter, Reynolds number and, most probably, nozzle-exit flow conditions. The jets of Bridges,[14] in particular, exhibit potential core lengths of about $z_c = 16.1r_0$ at $T_j = 0.84T_a$ and $z_c = 12.1r_0$ at $T_j = 1.72T_a$ in line with the LES findings, despite a diameter $D = 5.1$ cm which is five to ten times larger than that used in the simulations.

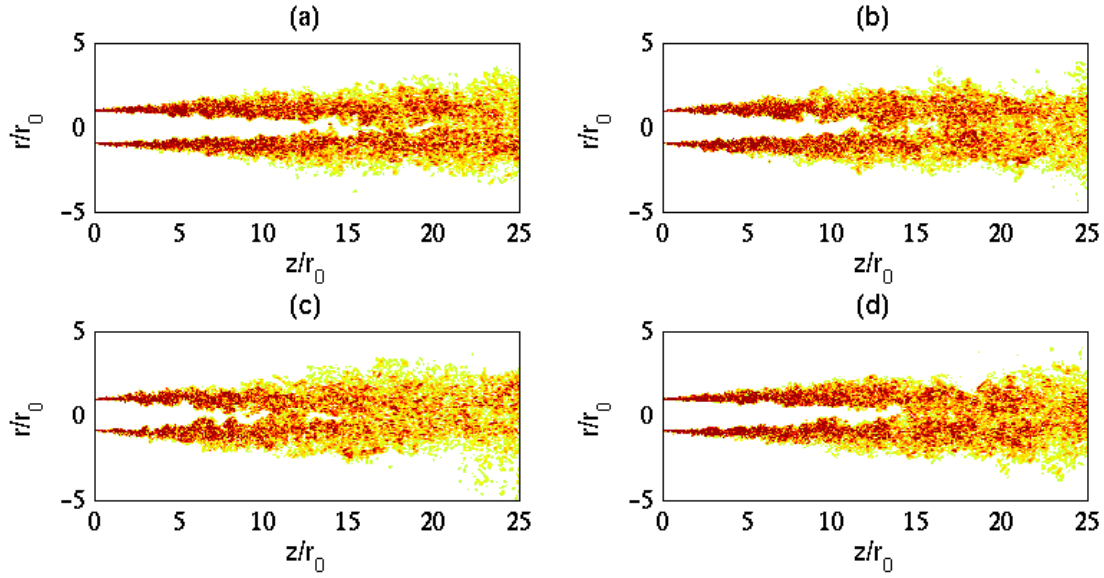

Figure 7. Snapshots in the (z, r) plane of vorticity norm $|\omega|$ for: (a) $T_j = T_a$ and $\mathrm{Re}_D = 10^5$, (b) $T_j = 1.5T_a$ and $\mathrm{Re}_D = 5 \times 10^4$, (c) $T_j = 2.25T_a$ and $\mathrm{Re}_D = 2.5 \times 10^4$, (d) $T_j = 1.5T_a$ and $\mathrm{Re}_D = 10^5$. The colour scale ranges up to the level of $6u_j/r_0$.

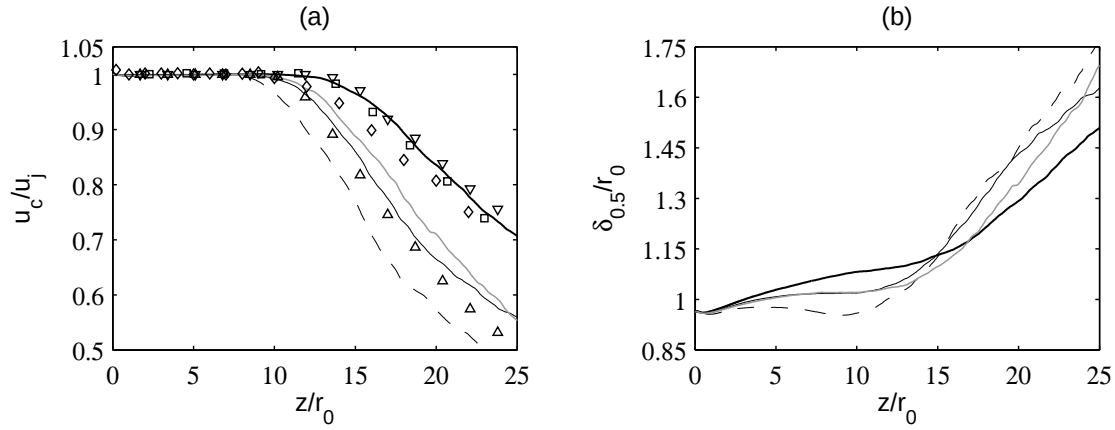

Figure 8. Variations (a) of centerline mean axial velocity u_c and (b) of jet half-width $\delta_{0.5}$ for: ——— $T_j = T_a$ and $\mathrm{Re}_D = 10^5$, ——— $T_j = 1.5T_a$ and $\mathrm{Re}_D = 5 \times 10^4$, – – – $T_j = 2.25T_a$ and $\mathrm{Re}_D = 2.5 \times 10^4$, ——— $T_j = 1.5T_a$ and $\mathrm{Re}_D = 10^5$; measurements for Mach number 0.9 jets at $\mathrm{Re}_D \geq 4 \times 10^5$: ▽ Bridges[14] ($T_j = 0.84T_a$), ◇ Fleury *et al.*[62] ($T_j = T_a$), □ Arakeri *et al.*[64] ($T_j = 1.1T_a$), △ Bridges[14] ($T_j = 1.76T_a$).

Table 5. Axial position of the end of the potential core z_c, and peak rms values of fluctuating velocities u'_z and u'_r on the jet axis.

T_j/T_a	Re_D	z_c/r_0	$<u'^2_z>^{1/2}/u_j$	$<u'^2_r>^{1/2}/u_j$
1	10^5	15.9	11.4%	9.4%
1.5	5×10^4	12.5	13.4%	10.9%
2.25	2.5×10^4	10.6	14.6%	10.8%
1.5	10^5	13.2	13.2%	10.4%

The variations of the centerline rms values of axial and radial fluctuating velocities are displayed in figures 9(a-b). As previously for the jet mean flow, the temperature effects appear stronger than the Reynolds number effects. With rising temperature, the peak turbulence intensities are reached at axial locations farther upstream, in agreement with the shortening of the jet potential core, and they increase appreciably. They are equal to 11.4% at $T_j = T_a$, about 13.3% at $T_j = 1.5T_a$, and 14.6% at $T_j = 2.25T_a$ for velocity u'_z, refer to table 5 for velocity u'_r. Similar trends were observed in the experiments of Lau,[6] Lepicovsky,[7] Kearney-Fischer *et al.*,[8] and Bridges.[14] The latter author, in particular, obtained on the centerline of Mach number 0.9 jets peak levels of axial velocity fluctuations varying from 14.8% of u_j at $T_j = 0.84T_a$ to 15.6% of u_j at $T_j = 1.76T_a$. These values do not match well those found in the present study, which may be due to different jet initial conditions. This is also not surprising in view of the significant dispersion of the measurements of turbulence intensities in jets, compare for instance the experimental data of Fleury *et al.*[62] and of Arakeri *et al.*[64] in figures 9(a-b).

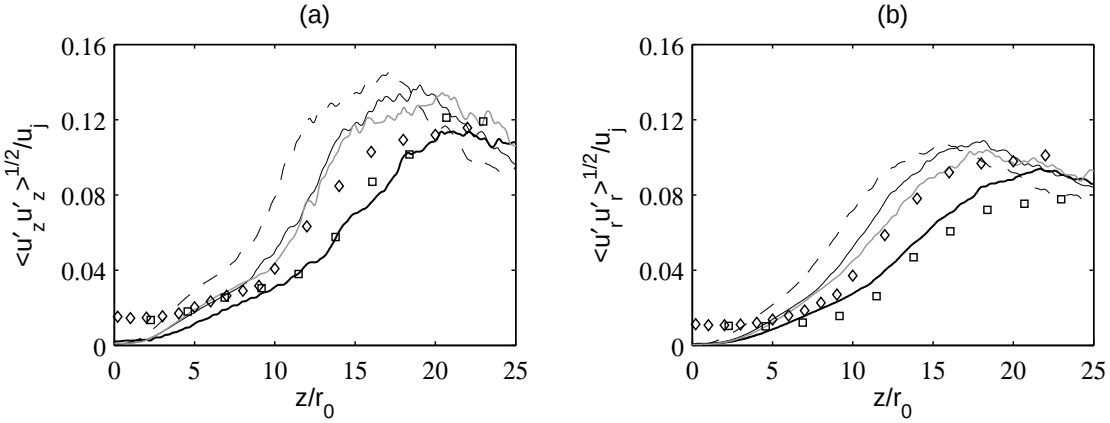

Figure 9. Variations of centerline rms values of fluctuating velocities (a) u'_z and (b) u'_r for: ——— $T_j = T_a$ and $\mathrm{Re}_D = 10^5$, ——— $T_j = 1.5T_a$ and $\mathrm{Re}_D = 5 \times 10^4$, – – – $T_j = 2.25T_a$ and $\mathrm{Re}_D = 2.5 \times 10^4$, ——— $T_j = 1.5T_a$ and $\mathrm{Re}_D = 10^5$; see caption of figure 8 for the symbols.

D. Acoustic fields

Snapshots of the near-field pressure fluctuations obtained directly by LES are represented in figures 10(a-d). Different trends as a function of temperature can be noted depending on the Reynolds number. With respect to the isothermal case in figure 10(a), the sound levels are visibly higher for the hot jets at decreasing Reynolds numbers in figure 10(b-c), whereas they seem to be lower for the hot jet at $\mathrm{Re}_D = 10^5$ in figure 10(d), especially in the sideline and upstream directions. Moreover, heating leads to the generation of additional pressure waves around $z = 3r_0$ in the mixing layers in the former case, but not in the latter. These waves are clearly distinguishable in figure 10(c) for the jet at $T_j = 2.25T_a$.

The far-field characteristics of the jets are examined based on the pressure signals calculated at a distance of 60 radii to the nozzle exit from the LES data at $r = 6.5r_0$ using the wave extrapolation method documented in section II.D. The overall sound pressure levels thus estimated at emission angles $30^o \leq \phi \leq 105^o$ relative to the jet direction are presented in figure 11(a). Compared to the measurements provided by Mollo-Christensen *et al.*,[65] Lush,[66] and Bogey *et al.*[67] for cold and isothermal jets at $\mathrm{M} = 0.9$ and $\mathrm{Re}_D \geq 5 \times 10^5$, scaled to the same distance to the nozzle, they all are 2-3 dB higher, which is expected[42] considering the lower Reynolds numbers of the present jets. There are, however, significant variations between the results of the simulations. Roughly speaking, it appears that rising temperature results in more noise for the jets of identical diameter, but in less noise at a fixed Reynolds number, as suggested by the pressure fields of figure 10.

To quantify the changes in noise intensity with heating, the differences between the overall sound levels of the hot jets and of the isothermal jet are plotted in figure 11(b) for $30^o \leq \phi \leq 105^o$ as previously, and reported in table 6 for the specific angles $\phi = 30^o$, 60^o, 90^o and 105^o. For the jets with identical diameter, a noise increase is found for $40^o \leq \phi \leq 70^o$ at $T_j = 1.5T_a$, and for $50^o \leq \phi \leq 80^o$ at $T_j = 2.25T_a$. It is notable in both cases around $\phi = 60^o$, where gains of +0.6 dB and +1.1 dB are obtained with respect to the isothermal jet. This radiation angle corresponds approximatively to that observed for the strong pressure waves originating from between $z = r_0$ and $z = 4r_0$ in the shear layers in figure 10(c), and is consistent

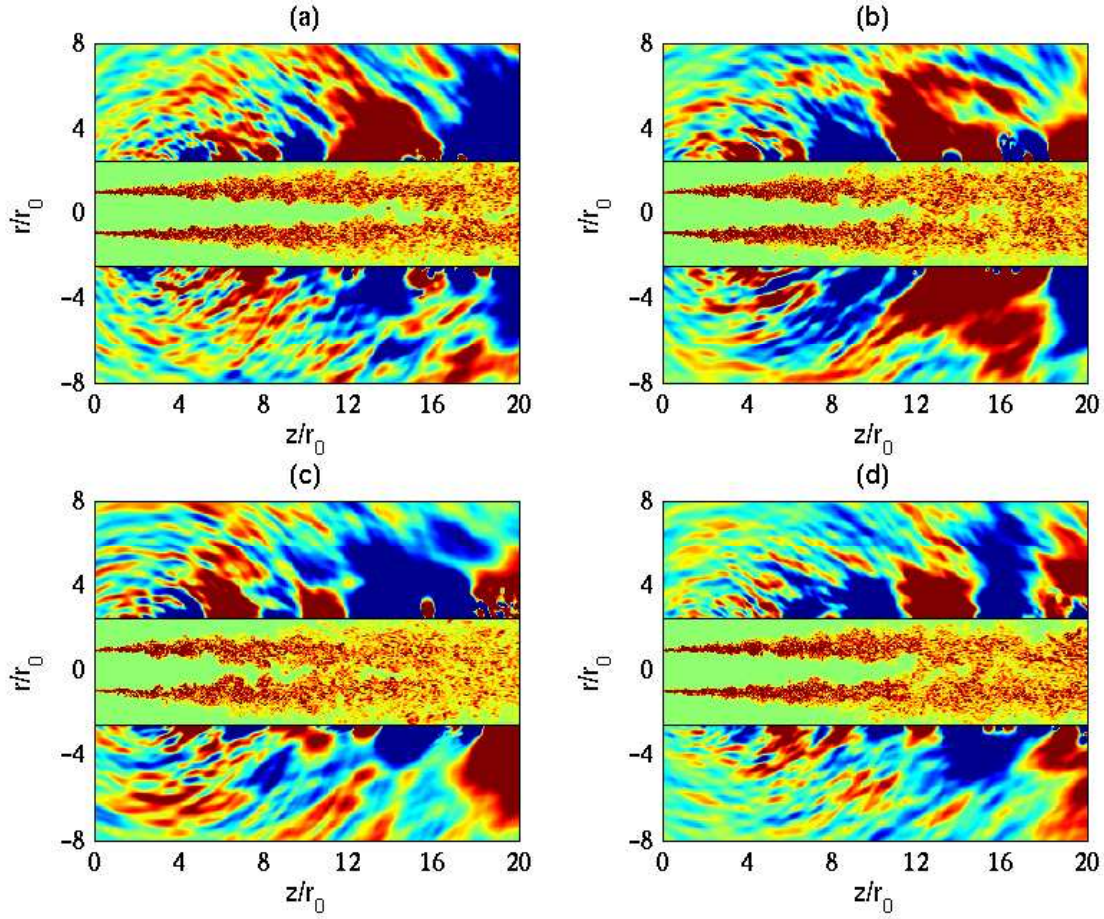

Figure 10. Snapshots in the (z, r) plane of vorticity norm $|\omega|$ in the flow and of fluctuating pressure $p - p_a$ outside, for: (a) $T_j = T_a$ and $\mathrm{Re}_D = 10^5$, (b) $T_j = 1.5T_a$ and $\mathrm{Re}_D = 5 \times 10^4$, (c) $T_j = 2.25T_a$ and $\mathrm{Re}_D = 2.5 \times 10^4$, (d) $T_j = 1.5T_a$ and $\mathrm{Re}_D = 10^5$. The colour scales range up to the level of $7u_j/r_0$ for the vorticity, and from -60 to 60 Pa for the pressure.

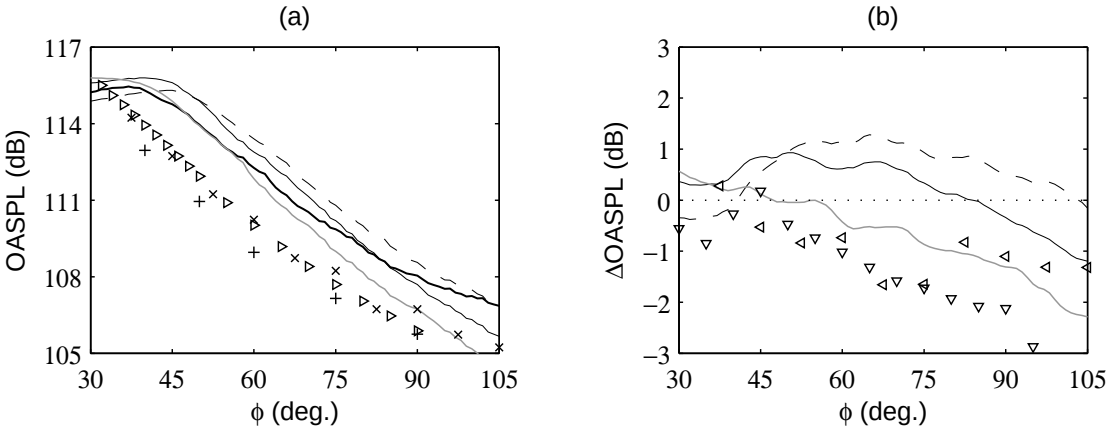

Figure 11. Representation as a function of the angle ϕ relative to the jet direction: (a) overall sound pressure levels (OASPL) at $60r_0$ from the nozzle exit for ——— $T_j = T_a$ and $\mathrm{Re}_D = 10^5$, ——— $T_j = 1.5T_a$ and $\mathrm{Re}_D = 5 \times 10^4$, – – – $T_j = 2.25T_a$ and $\mathrm{Re}_D = 2.5 \times 10^4$, ——— $T_j = 1.5T_a$ and $\mathrm{Re}_D = 10^5$; measurements for cold and isothermal jets at $\mathrm{M} = 0.9$ and $\mathrm{Re}_D \geq 5 \times 10^5$: + Mollo-Christensen *et al.*,[65] × Lush,[66] ▷ Bogey *et al.*;[67] (b) difference in OASPL (ΔOASPL) with respect to the isothermal case using same linetypes; ΔOASPL measured in far field for $\mathrm{M} = 0.9$ jets with $D = 5.1$ cm: ◁ between $T_j = 2.3T_a$ and $T_j = T_a$ in Tanna,[21] ▽ between $T_j = 1.43T_a$ and $T_j = 0.84T_a$ in Bridges & Wernet.[13]

Table 6. Difference in far-field overall sound pressure levels obtained between the M = 0.9 jets in the first column and those in the second column, at $\phi = 30^o$, 60^o, 90^o and 105^o. The second last and the last rows correspond to measurements of Tanna[21] and Bridges & Wernet,[13] respectively, for jets with $D = 5.1$ cm.

T_j/T_a, Re_D	T_j/T_a, Re_D	$\phi = 30^o$	$\phi = 60^o$	$\phi = 90^o$	$\phi = 105^o$
1.5, 5×10^4	1, 10^5	+0.4 dB	+0.6 dB	−0.3 dB	−1.2 dB
2.25, 2.5×10^4	1, 10^5	−0.3 dB	+1.1 dB	+0.7 dB	−0.2 dB
1.5, 10^5	1, 10^5	+0.6 dB	−0.5 dB	−1.3 dB	−2.3 dB
2.3, 2.6×10^5	1, 1.1×10^6	−0.4 dB	−0.7 dB	−1.1 dB	−1.3 dB
1.43, 5.8×10^5	0.84, 1.5×10^6	−0.5 dB	−1 dB	−2.1 dB	−3.2 dB

with the sound directivity of vortex pairing.[68,69] The noise increase is therefore most probably caused by interactions of large-scale vortical structures in the mixing-layer region, which are both more visible and more energy-containing when the Reynolds number Re_θ decreases from 943 at $T_j = T_a$ down to 254 at $T_j = 2.25T_a$, as shown in figures 3(a-c) and 5. In other words, it is due to Reynolds number effects.[42] These effects appear to be dominant around $\phi = 60^o$ as mentioned above, but not for $\phi \lesssim 40^o$ and $\phi \gtrsim 90^o$ where the sound levels of the hot jets do not substantially exceed those of the isothermal jet. For small and large emission angles, they are consequently counteracted by the classical effects of temperature on high subsonic jets, which are that heating reduces noise. This remark particularly applies to the angle $\phi = 105^o$, where losses of −1.2 dB and −0.2 dB happen with increasing temperature.

For the jet at $T_j = 1.5T_a$ and $\mathrm{Re}_D = 10^5$, a noise reduction is obtained with respect to the isothermal jet at nearly all emission angles. The hot jet is thus quieter, which is in line with experimental findings[18,21] for jets at Mach numbers greater than 0.7. This can be explained by the fact that at the high Reynolds numbers considered in experiments, the variations of viscosity have only a minor impact on results. The decrease of the sound levels is negligible in the vicinity of $\phi = 45^o$, and is progressively larger at wider radiation angles, as observed by Tanna[21] and Bridges & Wernet[13] for jets with a diameter $D = 5.1$ cm at an acoustic Mach number of 0.9. For a more quantitative comparison, the differences in sound level measured between jets at $T_j = 2.3T_a$ and $T_j = T_a$ by Tanna,[21] and between jets at $T_j = 1.43T_a$ and $T_j = 0.84T_a$ by Bridges & Wernet,[13] are depicted in figure 11(b), and given in table 6. The variations of the noise reduction with the emission angle in the computations and in the experiments are similar. The simulation data also lie between the measurements at $35^o \leq \phi \leq 45^o$ where noise reduction is weak or nonexistent, as well as at $\phi > 80^o$ where it is significant, with for instance −1.3 dB versus −1.1 dB and −2.1 dB at $\phi = 90^o$, and −2.3 dB versus −1.3 dB and −3.2 dB at $\phi = 105^o$. The disparities encountered here can be attributed to the differences in terms of temperature and Reynolds number, and to initial condition effects. In any case, temperature effects in agreement with those exhibited by laboratory-scale high-subsonic jets are captured in this study using LES, for the first time to the best of our knowledge.

The sound pressure spectra calculated at $60r_0$ from the nozzle exit at the angles $\phi = 30^o$, 60^o, 90^o and 105^o are represented in figures 12(a-d) as a function of Strouhal number $\mathrm{St}_D = fD/u_j$. Those obtained for cold and isothermal jets at M = 0.9 and $\mathrm{Re}_D \geq 7.8 \times 10^5$ by Tanna[21] and Bogey *et al.*[67] are also shown as references. As expected, discrepancies are observed because of the different temperatures and Reynolds numbers.

To describe the effects of temperature on noise components, the differences between the sound spectra of the hot jets and of the isothermal jet are displayed in figures 13(a-d). At $\phi = 30^o$, the hot jets all produce more noise at $0.15 \leq \mathrm{St}_D \leq 0.4$, but less noise at $\mathrm{St}_D \geq 0.6$. These opposite trends with heating, leading to stronger and weaker sound levels at low and high frequencies, respectively, in the downstream direction, are clearly found experimentally for jets at an acoustic Mach number of 0.5, refer to the paper by Tanna[21] and to the review by Tester & Morfey.[27] They are also noticed in the 1/3 octave spectra obtained by Tanna[21] at $\phi = 45^o$ for jets at M = 0.9, see also the discussion in Panda.[22] In the present hot jets, in addition, the narrow-banded noise increase centered around $\mathrm{St}_D = 0.25$ does not appear to depend appreciably on the temperature nor on the Reynolds number, whereas the broadband noise reduction at high frequencies becomes larger when the ratio T_j/T_a rises. At $\phi = 60^o$ in figure 13(b), the variations of the sound levels are smoother than previously. With heating, there is a noise increase at $\mathrm{St}_D \leq 0.7$, and no effect or a small decrease at $\mathrm{St}_D \geq 0.7$. The key factor here does not however seem to be the temperature, but the Reynolds number, since the lower the value of Re_D, the stronger the noise radiated by the jets for all spectral

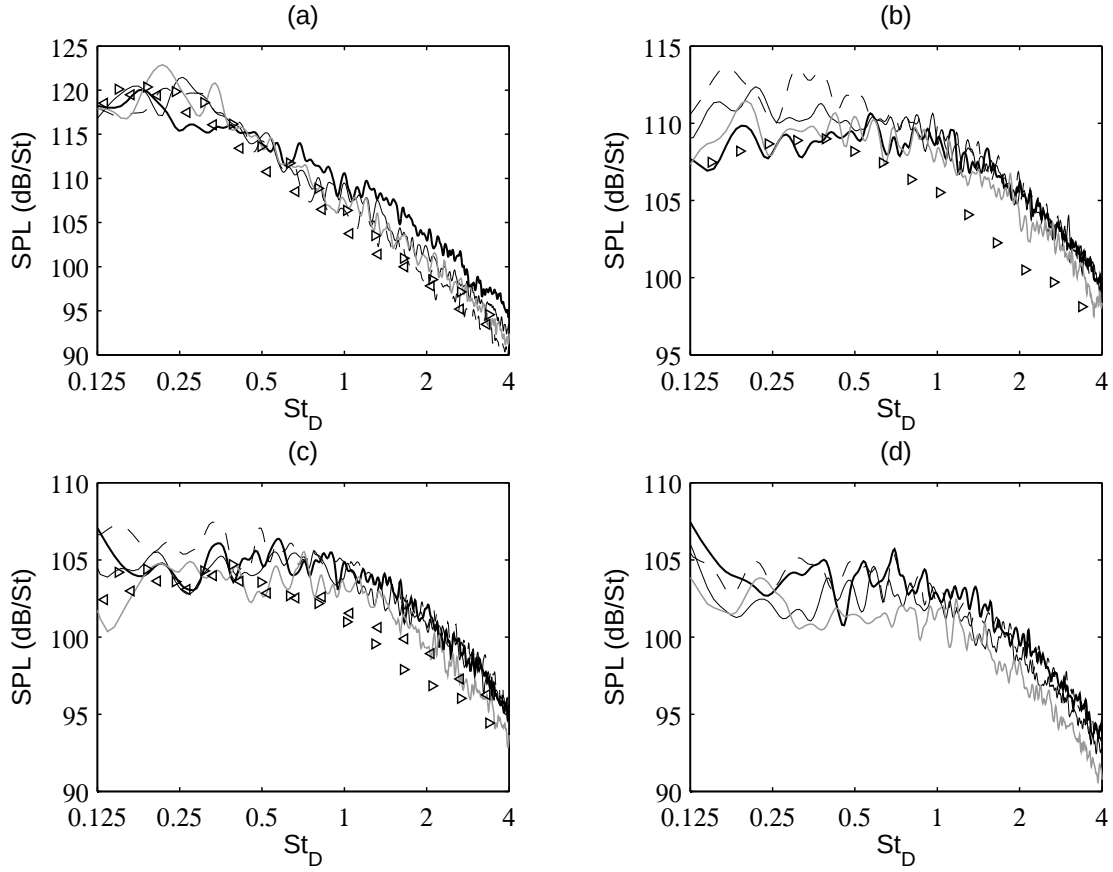

Figure 12. Sound pressure levels (SPL) at $60r_0$ from the nozzle exit at the angles ϕ of (a) 30°, (b) 60°, (c) 90° and (d) 105°, as a function of $\mathrm{St}_D = fD/u_j$, for: ——— $T_j = T_a$ and $\mathrm{Re}_D = 10^5$, ——— $T_j = 1.5T_a$ and $\mathrm{Re}_D = 5\times10^4$, – – – $T_j = 2.25T_a$ and $\mathrm{Re}_D = 2.5\times10^4$, ——— $T_j = 1.5T_a$ and $\mathrm{Re}_D = 10^5$; measurements for cold and isothermal jets at M = 0.9 and $\mathrm{Re}_D \geq 7.8\times10^5$: ◁ Tanna,[21] ▷ Bogey *et al.*[67]

components. This is not surprising given the conclusion reached above that the Reynolds number effects, resulting in the generation of extra pressure waves in the jet mixing layers, are dominant on the sound levels at $\phi = 60^o$. At $\phi = 90^o$ in figure 13(c), the graphs resemble those at $\phi = 60^o$, but the noise amplification at low frequencies is less pronounced. A nearly uniform noise reduction by about 1.5 dB is also found for the jet at $T_j = 1.5T_a$ and $\mathrm{Re}_D = 10^5$ for $\mathrm{St}_D \geq 0.5$. This tendency is similar to that observed experimentally at $\phi = 90^o$ between the M = 0.9 jets at $T_j = 0.84T_a$ and $T_j = 1.43T_a$ with $D = 5.1$ cm of Bridges & Wernet.[13] As illustrated in the figure, low-frequency acoustic components are nevertheless weakened by heating in the experiments, unlike the numerical findings. With values of Re_D equal to 10^5 in the simulations but greater than 5.8×10^5 in the jets of Bridges & Wernet,[13] this difference can be attributed to Reynolds number effects. Finally, at $\phi = 105^o$ in figure 13(d), the curves are relatively flat. The noise attenuation with respect to the isothermal case is very slight for the jet at $T_j = 2.25$, and is of about -1 dB for $T_j = 1.5T_a$ and $\mathrm{Re}_D = 5\times10^5$, and about -2 dB for $T_j = 1.5T_a$ and $\mathrm{Re}_D = 10^5$ for all frequencies.

In summary, four distinct changes stand out in the far-field pressure levels of the present jets at M= 0.9 with heating: an increase for $0.15 \leq \mathrm{St}_D \leq 0.4$ and a decrease for $\mathrm{St}_D \geq 0.6$ in the downstream direction, a strengthening for frequencies up to $\mathrm{St}_D = 0.7$ at emission angles $\phi \simeq 60^o$, and a reduction of all acoustic components in the upstream direction. It has been established that the extra noise at $\phi \simeq 60^o$ is caused by Reynolds number effects. The noise increase occurring at low frequencies in the downstream direction seems however to be insensitive to Reynolds number, which is in contradiction with the claims of Viswanathan.[26] At this point, the simulation results have not yet allowed us to identify its origin. The most likely scenario, according to the traditional view on temperature effects reassessed in Tester & Morfey,[27] is that heating generates additional temperature or entropy sources. One alternative involving no such sources would be that heating strongly modifies the subsonic jet noise component dominating in the downstream direction,

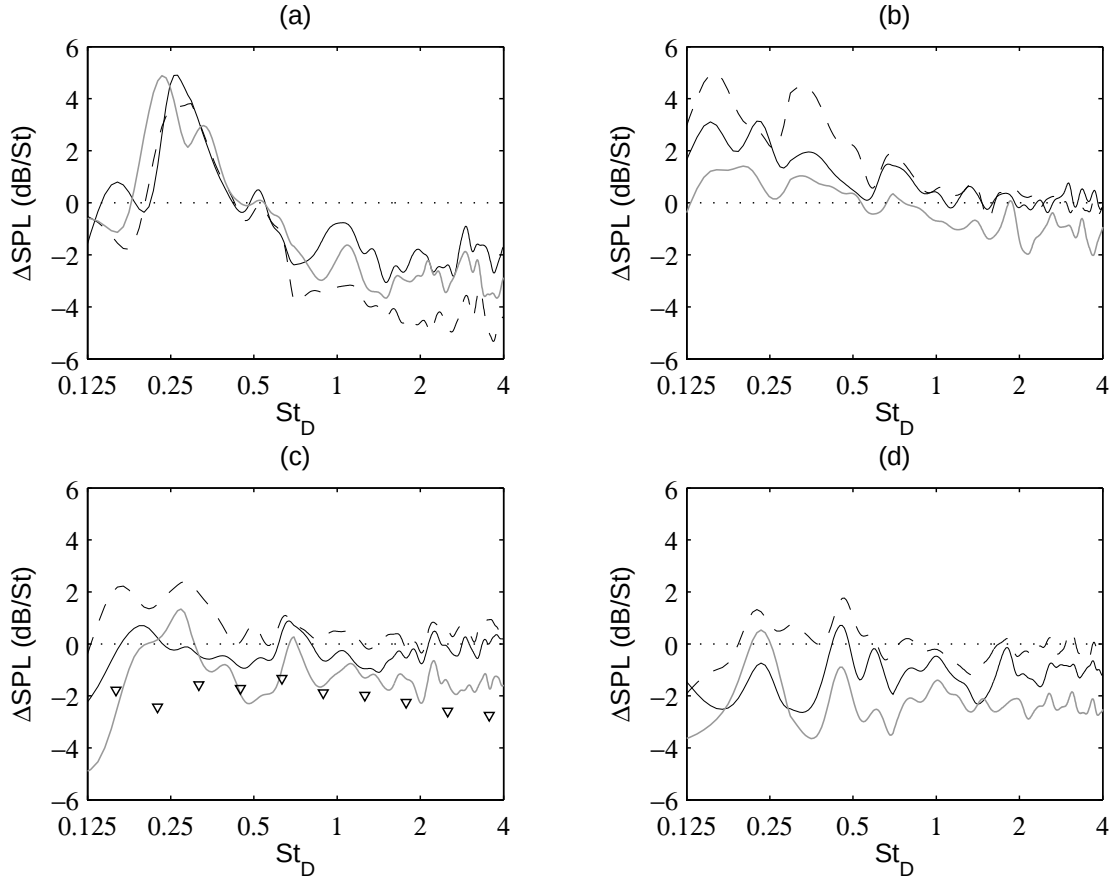

Figure 13. Difference in SPL (ΔSPL) at $60r_0$ from the nozzle exit at (a) $\phi = 30^o$, (b) 60^o, (c) 90^o and (d) 105^o, as a function of St_D, between the jets at ——— $T_j = 1.5T_a$ and $Re_D = 5 \times 10^4$, – – – $T_j = 2.25T_a$ and $Re_D = 2.5 \times 10^4$, ——— $T_j = 1.5T_a$ and $Re_D = 10^5$, and the isothermal jet; ΔSPL measured in far field for M = 0.9 jets with $D = 5.1$ cm: ▽ between $T_j = 1.43T_a$ and $T_j = 0.84T_a$ in Bridges & Wernet.[13]

associated with large-scale structures developing at the end of the potential core.[70–73] It is hoped that further analyses of the present results will be enlightening on this issue.

IV. Conclusion

The influence of temperature on initially highly disturbed jets at an acoustic Mach number M = 0.9 has been investigated using LES for round jets with similar nozzle-exit conditions at temperatures $T_j = T_a$, $T_j = 1.5T_a$ and $T_j = 2.25T_a$ and Reynolds numbers $2.5 \times 10^4 \leq \mathrm{Re}_D \leq 10^5$. Jets with the same diameter as well as jets at an identical $\mathrm{Re}_D = 10^5$ have been considered, in order to distinguish between the temperature effects and the Reynolds number effects due to the increase of molecular viscosity with heating. The trends exhibited for the aerodynamic and acoustic fields of the jets with rising temperature are in good agreement with experimental results. For the jets at a constant Re_D, in particular, an overall noise reduction is noted, in the same way as in experiments for jets at M > 0.7 and at Re_D typically greater than 4×10^5. The variations of the sound levels with temperature, depending on the radiation angle and frequency, are also consistent with corresponding measurements. This is the first time, as far as we know, that this is successfully achieved in a computational study.

In this work, the Reynolds number effects due to heating, observed only for the jets with the same diameter hence at decreasing Re_D, mainly result in a faster spreading of the mixing layers, and in higher turbulence intensities and stronger large-scale structures downstream of the nozzle. These structures and their mutual interactions generate additional noise components between $\phi \simeq 45^o$ and $\phi \simeq 75^o$. The temperature effects, obtained in all cases whatever the value of Re_D, consist of a shorter potential core followed by a more rapid

jet development and of higher velocity fluctuation levels on the jet axis. Concerning their impact on the acoustic field, they lead to a reduction of high-frequency noise components in the downstream direction, and of all components in the upstream direction. More interestingly, an extra hump centered around $\mathrm{St}_D = 0.25$ is found to emerge in the far-field pressure spectra at $\phi \simeq 30^o$, as is the case in most experiments for heated subsonic jets. This temperature effect is generally attributed to the creation of extra dipole sources associated with entropy fluctuations, but is still a matter of debate, particularly because of questions about experimental jet noise databases. With regards to this point, it is interesting to emphasize that the extra hump at low frequencies captured in the present simulations of hot jets does not appear to be due to Reynolds number effects. It is also unlikely to be caused by a contamination by an internal noise, nor by initial conditions effects because of the carefully controlled conditions in the LES.

Acknowledgments

This work was granted access to the HPC resources of CINES (Centre Informatique National de l'Enseignement Supérieur) and IDRIS (Institut du Développement et des Ressources en Informatique Scientifique) under the allocation 2012-020204 made by GENCI (Grand Equipement National de Calcul Intensif).

References

[1]Maslowe, S.A. and Kelly, R.E., "Inviscid instability of an unbounded heterogeneous shear layer," *J. Fluid Mech.*, Vol. 48, No. 2, 1971, pp. 405-415.

[2]Michalke, A., "Survey on jet instability theory," *Prog. Aerospace Sci.*, Vol. 21, 1984, pp. 159-199.

[3]Davey, R.F. and Roshko, A., "The effect of a density difference on shear-layer instability," *J. Fluid Mech.*, Vol. 53, No. 3, 1972, pp. 523543.

[4]Brown, G.L. and Roshko, A., "On density effect and large structure in turbulent mixing layers," *J. Fluid Mech.*, Vol. 64, No. 4, 1974, pp. 775816.

[5]Witze, P.O., "Centerline velocity decay of compressible free jets," *AIAA J.*, Vol. 12, No. 4, 1974, pp. 417-418.

[6]Lau, J.C., "Effects of exit Mach number and temperature on mean-flow and turbulence characteristics in round jets," *J. Fluid Mech.*, Vol. 105, 1981, pp. 193-218.

[7]Lepicovsky, J., "Experimental research on mixing enhancement in heated free jet flows," *3rd ASME/JSME Joint Fluids Engineering Conference*, 18-23 July 1999, San Francisco, CA, USA, No. FEDSM99-7247.

[8]Kearney-Fischer, M., Kim, J.-H., and Samimy, M., "Control of a high Reynolds number Mach 0.9 heated jet using plasma actuators," *Phys. Fluids*, Vol. 21, No. 9, 2009, 095101.

[9]Pitts, W.M., "Effects of global density ratio on the centerline mixing behavior of axisymmetric turbulent jets," *Exp. Fluids*, Vol. 11, 1991, pp. 125-134.

[10]Russ, S. and Strykowski, P.J., "Turbulent structure and entrainment in heated jets: The effect of initial conditions," *Phys. Fluids A*, Vol. 5, No. 12, 1993, pp. 3216-3225.

[11]Amielh, M., Djeridane, T., Anselmet, F., and Fulachier, L., "Velocity near-field of variable density turbulent jets," *Int. J. Heat Mass Transfer*, Vol. 39, No. 10, 1996, pp. 2149-2164.

[12]Bridges, J. and Wernet, M., "Measurements of the aeroacoustic sound source in hot jets," AIAA Paper 2003-3130, 2003.

[13]Bridges, J. and Wernet, M.P., "Effect of temperature on jet velocity spectra," AIAA Paper 2007-3628, 2007.

[14]Bridges, J., "Effect of heat on space-time correlations in jets," AIAA Paper 2006-2534, 2006.

[15]Lassiter, L.W. and Hubbard, H.H., "Experimental studies of noise from subsonic jets in still air," NACA TN-2757, 1952.

[16]Plumbee, H.E., Wynne, G.A., and Zinn, B.T., "Effect of jet temperature on jet and pure tone radiation," NASA CR-1472, 1969.

[17]Rollin, V.G., "Effect of jet temperature on jet noise generation," NACA TN-4217, 1958.

[18]Fisher, M.J., Lush, P.A., and Harper-Bourne, M., "Jet noise," *J. Sound Vib.*, Vol. 28, No. 3, 1973, pp. 563-585.

[19]Hoch, R.G., Duponchel, J.P., Cocking, B.J., and Bryce, W.D., "Studies of the influence of density on jet noise," *J. Sound Vib.*, Vol. 28, No. 4, 1973, pp. 649-668.

[20]Tanna, H.K., Dean, P.D., and Fisher, M.J., "The influence of temperature on shock-free supersonic jet noise," *J. Sound Vib.*, Vol. 39, No. 4, 1975, pp. 429-460.

[21]Tanna, H.K., "An experimental study of jet noise. Part I: Turbulent mixing noise," *J. Sound Vib.*, Vol. 50, No. 3, 1977, pp. 405-428.

[22]Panda, J., "Experimental investigation of turbulent density fluctuations and noise generation from heated jets," *J. Fluid Mech.*, Vol. 591, 2007, pp. 73-96.

[23]Morfey, C.L., "Amplification of aerodynamic noise by convected flow inhomogeneities," *J. Sound Vib.*, Vol. 31, No. 4, 1973, pp. 391-397.

[24]Tester, B.J. and Morfey, C.L., "Developments in jet noise modelling - Theoretical predictions and comparisons with measured data," *J. Sound Vib.*, Vol. 46, No. 1, 1976, pp. 79-103.

[25]Morfey, C.L., Szewczyk, V.M., and Tester, B.J., "New scaling laws for hot and cold jet mixing noise based on a geometric acoustics model," *J. Sound Vib.*, Vol. 61, No. 2, 1978, pp. 255-292.

[26]Viswanathan, K., "Aeroacoustics of hot jets," *J. Fluid Mech.*, Vol. 516, 2004, pp. 39-82.

[27]Tester, B.J. and Morfey, C.L., "Jet mixing noise: a review of single stream temperature effects," AIAA Paper 2009-3376, 2009.

[28]Harper-Bourne, M., "Jet noise measurements: past and present," *Int. J. of Aeroacoustics*, Vol. 9, No. 4 & 5, 2010, pp. 559-588.

[29]Bridges, J. and Brown, C.A., "Validation of the small hot jet acoustic rig for aeroacoustics," AIAA Paper 2005-2846, 2005.

[30]Zaman, K.B.M.Q., "Effect of initial boundary-layer state on subsonic jet noise," *AIAA J.*, Vol. 50, No. 8, 2012, pp. 1784-1795.

[31]Karon, A.Z. and Ahuja, K.K., "Effect of nozzle-exit boundary layer on jet noise," AIAA Paper 2013-0615, 2013.

[32]Bogey, C. and Bailly, C., "Influence of nozzle-exit boundary-layer conditions on the flow and acoustic fields of initially laminar jets," *J. Fluid Mech.*, Vol. 663, 2010, pp. 507-539.

[33]Bogey, C., Marsden, O., and Bailly, C., "Influence of initial turbulence level on the flow and sound fields of a subsonic jet at a diameter-based Reynolds number of 10^5," *J. Fluid Mech.*, Vol. 701, 2012, pp. 352-385.

[34]Bogey, C. and Marsden, O., "Identification of the effects of the nozzle-exit boundary-layer thickness and its corresponding Reynolds number in initially highly disturbed subsonic jets," to appear in *Phys. Fluids*, Vol. 25, 2013.

[35]Wang, P., Fröhlich, J., Michelassi, V., and Rodi, W., "Large-eddy simulation of variable-density turbulent axisymmetric jets," *Int. J. Heat and Fluid Flow*, Vol. 29, No. 3, 2008, pp. 654-664.

[36]Foysi, H., Mellado, J.P., and Sarkar, S., "Large-eddy simulation of variable-density round and plane jets," *Int. J. Heat and Fluid Flow*, Vol. 31, No. 3, 2010, pp. 307-314.

[37]Colonius, T. and Lele, S.K., "Computational aeroacoustics: progress on nonlinear problems of sound generation," *Progress in Aerospace Sciences*, Vol. 40, 2004, pp. 345-416.

[38]Bailly, C. and Bogey, C., "Contributions of CAA to jet noise research and prediction," *Int. J. Comput. Fluid Dyn.*, Vol. 18, No. 6, 2004, pp. 481-491.

[39]Wang, M., Freund J.B., and Lele, S.K., "Computational prediction of flow-generated sound," *Annu. Rev. Fluid. Mech.*, Vol. 38, 2006, pp. 483-512.

[40]Bogey, C., Marsden, O., and Bailly, C., "Large-Eddy Simulation of the flow and acoustic fields of a Reynolds number 10^5 subsonic jet with tripped exit boundary layers," *Phys. Fluids*, Vol. 23, No. 3, 2011, 035104.

[41]Bogey, C., Marsden, O., and Bailly, C., "On the spectra of nozzle-exit velocity disturbances in initially nominally turbulent jets," *Phys. Fluids*, Vol. 23, No. 9, 2011, 091702.

[42]Bogey, C., Marsden, O., and Bailly, C., "Effects of moderate Reynolds numbers on subsonic round jets with highly disturbed nozzle-exit boundary layers," *Phys. Fluids*, Vol. 24, No. 10, 2012, 105107.

[43]Fortuné, V., Lamballais, E., and Gervais, Y., "Noise radiated by a non-isothermal, temporal mixing layer. Part I: Direct computation and prediction using compressible DNS," *Theoret. Comput. Fluid Dynamics*, Vol. 18, No. 1, 2004, pp. 61-81.

[44]Sharma, A. and Lele, S.K., "Effects of heating on noise radiation from turbulent mixing layers with initially laminar and turbulent boundary layers," AIAA Paper 2012-1168, 2012.

[45]Lesshafft, L., Huerre, P. and Sagaut, P., "Aerodynamic sound generation by global modes in hot jets" *J. Fluid Mech.*, Vol. 647, 2010, pp. 473-489.

[46]Bodony, D.J. and Lele, S.K., "On using large-eddy simulation for the prediction of noise from cold and heated turbulent jets," *Phys. Fluids*, Vol. 17, No. 8, 2012, 085103.

[47]Zaman, K.B.M.Q., "Effect of initial condition on subsonic jet noise," *AIAA J.*, Vol. 23, 1985, pp. 1370-1373.

[48]Zaman, K.B.M.Q., "Far-field noise of a subsonic jet under controlled excitation," *J. Fluid Mech.*, Vol. 152, 1985, pp. 83-111.

[49]Mohseni, K. and Colonius, T., "Numerical treatment of polar coordinate singularities," *J. Comput. Phys.*, Vol. 157, No. 2, 2000, pp. 787-795.

[50]Bogey, C., de Cacqueray, N., and Bailly, C., "Finite differences for coarse azimuthal discretization and for reduction of effective resolution near origin of cylindrical flow equations," *J. Comput. Phys.*, Vol. 230, No. 4, 2011, pp. 1134-1146.

[51]Bogey, C. and Bailly, C., "A family of low dispersive and low dissipative explicit schemes for flow and noise computations," *J. Comput. Phys.*, Vol. 194, No. 1, 2004, pp. 194-214.

[52]Bogey, C., de Cacqueray, N., and Bailly, C., "A shock-capturing methodology based on adaptative spatial filtering for high-order non-linear computations," *J. Comput. Phys.*, Vol. 228, No. 5, 2009, pp. 1447-1465.

[53]Berland, J., Bogey, C., Marsden, O., and Bailly, C., "High-order, low dispersive and low dissipative explicit schemes for multi-scale and boundary problems," *J. Comput. Phys.*, Vol. 224, No. 2, 2007, pp. 637-662.

[54]Tam, C.K.W and Dong, Z., "Radiation and outflow boundary conditions for direct computation of acoustic and flow disturbances in a nonuniform mean flow., *J. Comput. Acoust.*, Vol. 4, No. 2,, 1996, pp. 175201.

[55]Bogey, C. and Bailly, C., "Three-dimensional non reflective boundary conditions for acoustic simulations: far-field formulation and validation test cases," *Acta Acustica*, Vol. 88, No. 4, 2002, pp. 463-471.

[56]Bogey, C. and Bailly, C., "Large Eddy Simulations of transitional round jets: influence of the Reynolds number on flow development and energy dissipation," *Phys. Fluids*, Vol. 18, No. 6, 2006, 065101.

[57]Bogey, C. and Bailly, C., "Turbulence and energy budget in a self-preserving round jet: direct evaluation using large-eddy simulation," *J. Fluid Mech.*, Vol. 627, 2009, pp. 129-160.

[58]Fauconnier, D., Bogey, C., and Dick, E., "On the performance of relaxation filtering for large-eddy simulation," *J. Turbulence*, Vol. 14, No. 1, 2013, pp. 22-49.

[59]Bogey, C., Barré, S., Juvé, D., and Bailly, C., "Simulation of a hot coaxial jet : direct noise prediction and flow-acoustics correlations," *Phys. Fluids*, Vol. 21, No. 3, 2009, 035105.

[60]Ahuja, K.K., Tester, B.J., and Tanna, H.K., "Calculation of far field jet noise spectra from near field measurements with true source location," *J. Sound Vib.*, Vol. 116, No. 3, 1987, pp. 415-426.

[61]Davies, P.O.A.L., Fisher, M.J., and Barratt, M.J., "The characteristics of the turbulence in the mixing region of a round jet," *J. Fluid Mech.*, Vol. 15, 1963, pp. 337-367.

[62]Fleury, V., Bailly, C., Jondeau, E., Michard, M., and Juvé, D., "Space-time correlations in two subsonic jets using dual-PIV measurements," *AIAA J.*, Vol. 46, No. 10, 2008, pp. 2498-2509.

[63]Wernet, M.P., "Temporally resolved PIV for space-time correlations in both cold and hot jet flows," *Meas. Sci. Technol.*, Vol. 18, No. 5, 2007, pp. 1387-1403.

[64]Arakeri, V.H., Krothapalli, A., Siddavaram, V., Alkislar, M.B., and Lourenco, L., "On the use of microjets to suppress turbulence in a Mach 0.9 axisymmetric jet," *J. Fluid Mech.*, Vol. 490, 2003, pp. 75-98.

[65]Mollo-Christensen, E., Kolpin, M.A., and Martucelli, J.R., "Experiments on jet flows and jet noise far-field spectra and directivity patterns," *J. Fluid Mech.*, Vol. 18, No. 2, 1964, pp. 285-301.

[66]Lush, P.A., "Measurements of subsonic jet noise and comparison with theory," *J. Fluid Mech.*, Vol. 46, No. 3, 1971, pp. 477-500.

[67]Bogey, C., Barré, S., Fleury, V., Bailly, C., and Juvé, D., "Experimental study of the spectral properties of near-field and far-field jet noise," *Int. J. of Aeroacoustics*, Vol. 6, No. 2, 2007, pp. 73-92.

[68]Colonius, T., Lele, S.K., and Moin, P., "Sound generation in a mixing layer," *J. Fluid Mech.*, Vol. 330, 1997, pp. 375-409.

[69]Bogey, C., Bailly, C., and Juvé, D., "Numerical simulation of the sound generated by vortex pairing in a mixing layer," *AIAA J.*, Vol. 38, No. 12, 2000, pp. 2210-2218.

[70]Tam, C.K.W., "Jet noise: since 1952," *Theoret. Comput. Fluid Dynamics*, Vol. 10, 1998, pp. 393-405.

[71]Panda, J., Seasholtz, R.G., and Elam, K.A., "Investigation of noise sources in high-speed jets via correlation measurements," *J. Fluid Mech.*, Vol. 537, 2005, pp. 349-385.

[72]Bogey, C. and Bailly, C., "An analysis of the correlations between the turbulent flow and the sound pressure field of subsonic jets," *J. Fluid Mech.*, Vol. 583, 2007, pp. 71-97.

[73]Tam, C.K.W., Viswanathan, K., Ahuja, K.K., and Panda, J., "The sources of jet noise: experimental evidence," *J. Fluid Mech.*, Vol. 615, 2008, p. 253-292.